# Selective Coupling Enhances Harmonic Generation of Whispering-Gallery Modes

Luke S. Trainor,[1] Florian Sedlmeir,[1,2] Christian Peuntinger,[1] and Harald G. L. Schwefel[1,*]
[1]*The Dodd-Walls Centre for Photonic and Quantum Technologies, Department of Physics, University of Otago, 730 Cumberland Street, Dunedin 9016, New Zealand*
[2]*Max Planck Institute for the Science of Light, Staudtstraße 2, 90158 Erlangen, Germany*

(Received 27 September 2017; published 7 February 2018)

We demonstrate second-harmonic generation (SHG) in an *x*-cut congruent lithium niobate (LN) whispering-gallery mode (WGM) resonator. First, we show theoretically that independent control of the coupling of the pump and signal modes is optimal for high conversion rates. A coupling scheme based on our earlier work [F. Sedlmeir *et al.*, Phys. Rev. Applied **7**, 024029 (2017)] is then implemented experimentally to verify this improvement. Thereby, we are able to improve on the efficiency of SHG by more than an order of magnitude by selectively outcoupling using a LN prism, utilizing the birefringence of it and the resonator in kind. This method is also applicable to other nonlinear processes in WGM resonators.

DOI: 10.1103/PhysRevApplied.9.024007

## I. INTRODUCTION

Second-harmonic generation (SHG) was one of the first nonlinear processes to be observed after the invention of the laser [1]. It has found wide use in the frequency doubling of lasers and makes hard-to-reach frequency domains more accessible. However, SHG is dictated by weak second-order nonlinear susceptibility, and it hence usually requires high-power pump lasers. In order to increase the process's efficiency, a cavity can be used, e.g., by placing the nonlinear crystal inside a bow-tie resonator. Such a method can be very efficient, but it requires specially coated mirrors which limit the bandwidth of the operation and are bulky and expensive to set up. Recent monolithic implementations [2,3] have achieved high conversion efficiencies by resonantly confining the interacting light fields within a whispering-gallery mode (WGM) resonator [4].

WGM resonators are natural vessels to study nonlinear effects due to an unparalleled combination of favorable characteristics [5,6]. The method of entrapment is total internal reflection, which allows for very good spatial confinement along the rim of the resonator. Furthermore, total internal reflection is only very weakly dependent on the wavelength of light, which allows a large range of wavelengths to be simultaneously resonant in the same cavity; the range depends solely on the absorbency of the bulk dielectric. These attributes allow for resonances with very high $Q$ factors and finesse, greatly enhancing the contained fields—and hence the nonlinear effects of the bulk medium. The efficiency is high as both the pump and the harmonic light can be resonantly enhanced and propagate with the same phase velocity within the WGM resonator. This phase matching can be achieved in some birefringent nonlinear crystals and is highly dependent on the exact dispersion of the crystal. By the chance of nature, some crystals allow natural phase matching for SHG, albeit in very limited frequency domains [2,3]. Slightly broader operation is afforded through periodic poling of the crystal [7]. An elegant method for broadband operation is to use the WGM in a distinct crystal orientation, namely, the *x* cut (or *y* cut), where the optic axis of a uniaxial birefringent crystal lies within the plane of the equator [8]. In such a system, the refractive index of the transverse-magnetic (TM) mode—in addition to the effective nonlinear susceptibility—oscillates as the light propagates around the resonator's rim. This oscillating refractive index allows broadband phase matching at slightly reduced efficiency [9,10]. Although such WGM implementations still can be highly efficient, they are intrinsically limited by the external coupling rate of the harmonic light. Coupling to WGMs is usually achieved by overlapping the evanescent field of the resonator with the evanescent field of, e.g., a prism. Therefore, typically either the pump is overcoupled or the signal is undercoupled, as the evanescent field decay length scales with the wavelength. The maximum of the prism outcoupled harmonic power does not coincide with the maximum intrinsic harmonic light. By exploiting the birefringence of the WGM and the coupling prism, it is, however, possible to independently control the coupling rates for pump and second-harmonic modes, thereby selectively outcoupling the light.

In a previous work, we developed the theoretical model for selective coupling and demonstrated it in the linear regime [11]. In this article, we show experimentally that this method can improve SHG conversion efficiency by

*harald.schwefel@otago.ac.nz

 

more than an order of magnitude in an $x$-cut resonator. These results also apply to $z$-cut resonators.

## II. SELECTIVE COUPLING

In order to quantify the selective coupling, we introduce the quality factor $Q$. The $Q$ factors of WGMs are determined by the resonance frequency, $\omega$, in addition to the linewidth, $\Delta\omega$. The linewidth can be attributed to the intrinsic loss rate, $\gamma^0$, from absorption in the resonator, and the coupling rate, $\gamma^c$, into and out of the resonator. Each of these rates partially contributes to the total linewidth, and hence inversely to the $Q$ factor:

$$\frac{1}{Q} = \frac{\Delta\omega}{\omega} = \frac{2(\gamma^0 + \gamma^c)}{\omega} = \frac{1}{Q^0} + \frac{1}{Q^c}. \tag{1}$$

Typically, the intrinsic loss rate is fixed (by the bulk dielectric absorption and surface scattering). The coupling rate, however, is dependent only on the coupling mechanism used; in the case of WGMs, this is evanescent coupling, which has exponential distance dependence [12]. Therefore, by moving the coupler with respect to the resonator, we can continuously adjust the coupling rate. This is important, as the maximum intracavity power is reached when $\gamma^c = \gamma^0$. This condition is known as *critical coupling*.

Critical coupling of the pump, however, does not ensure that the second harmonic is also critically coupled. The distance over which the evanescent field decays is dependent on the mode's wavelength. For example, it has been shown [12] that the coupling rate to a WGM resonator using prism coupling in air is

$$\gamma^c \propto \sqrt{\lambda} e^{-2\kappa d}, \quad \text{where } \kappa \approx \frac{2\pi}{\lambda}\sqrt{n_r^2 - 1}, \tag{2}$$

where $n_r$ is the effective refractive index for the mode, $d$ is the distance between the prism and the resonator, and $\lambda$ is the vacuum wavelength of the mode. Accordingly, the coupling rates for SHG and the pump are—in general—different. For example, for high-$Q$ resonances, the intrinsic loss rate is very small, so critical coupling is reached at small coupling rates. In this case, the exponential term dominates and the pump couples critically at a much greater distance than the signal.

In the next section, we show—using a simple application of coupled-mode theory—that simultaneous critical coupling of both fields is optimal for SHG. The rate equations for SHG in a cavity can be written as [13]

$$\frac{dA_p}{dt} = -\Gamma_p A_p - iKA_p^* A_s + F_p, \tag{3}$$

$$\frac{dA_s}{dt} = -\Gamma_s A_s - 2iKA_p^2, \tag{4}$$

where subscript $s$ and $p$ represent signal (second-harmonic) and pump modes; $A$ is the slowly varying amplitude of the mode; $\Gamma = \gamma^c + \gamma^0 - i\delta\omega$, where $\delta\omega$ is the detuning from the resonance; and $K$ is the second-harmonic coupling coefficient. To use coupled-mode theory, the amplitudes must be normalized to energy, so naturally we choose $|A|^2 = W$, where $W$ is the energy stored in the mode. With this normalization, the pump force is $F_p = \sqrt{2\gamma_p^c} S_p$, where $S_p$ is the pump source amplitude, which satisfies $|S_p|^2 = P_{\text{incident}}$ for the incident pump power. This relation connects the incoming pump field with the intracavity fields.

In our experiment, we assume that the system has reached a steady state, and that we can use the undepleted pump approximation ($iKA_p^* A_s \approx 0$), whence we find for the intracavity SHG field (while assuming we are not detuned from the resonances, $\delta\omega_{p,s} = 0$)

$$A_s = -2iK \frac{2\gamma_p^c}{(\gamma_p^c + \gamma_p^0)^2(\gamma_s^c + \gamma_s^0)} P_{\text{incident}}. \tag{5}$$

The outcoupled second-harmonic power is then given by $P_{\text{SHG}} = |\sqrt{2\gamma_s^c} A_s|^2$; hence,

$$P_{\text{SHG}} = 32K^2 \frac{(\gamma_p^c)^2 \gamma_s^c}{(\gamma_p^c + \gamma_p^0)^4 (\gamma_s^c + \gamma_s^0)^2} P_{\text{incident}}^2. \tag{6}$$

For a given pump power and fixed intrinsic loss rates, the maximum of this function is reached when both pump and signal are critically coupled ($\gamma_{p,s}^c = \gamma_{p,s}^0$).

Here, there is thus a trade-off, which we illustrate in Fig. 1. To create this figure, a diamond prism is used to couple transverse-electric (TE) light of 1548.36 nm into an $x$-cut congruent lithium niobate (LN) WGM resonator. This prism can be moved by a piezoelectric linear stage closer to or farther from the resonator. The pump's second harmonic is generated as a TM mode inside the resonator. To ensure maximum conversion of the pump, it needs to be critically coupled. However, to obtain the most useful outcoupled second-harmonic power, the second harmonic should be critically coupled. This occurs when the prism is much closer to the resonator, due both to the increased decay in Eq. (2) and to the fact that TM modes couple more poorly in general [14]. If we could achieve the best conversion and best signal coupling simultaneously, then we would improve the second-harmonic output. For a more detailed description of this experiment, see Sec. III A.

This is where selective coupling comes in. By adding an additional coupler, which only couples to the second harmonic, we can maintain critical coupling of the pump while *at the same time* critically coupling the second harmonic.

As we see in Fig. 1, critical coupling of both the signal and the pump is normally not possible. However, in Fig. 2, we show how it is possible to selectively couple to TM modes in an $x$-cut scheme for a negative uniaxial crystal.

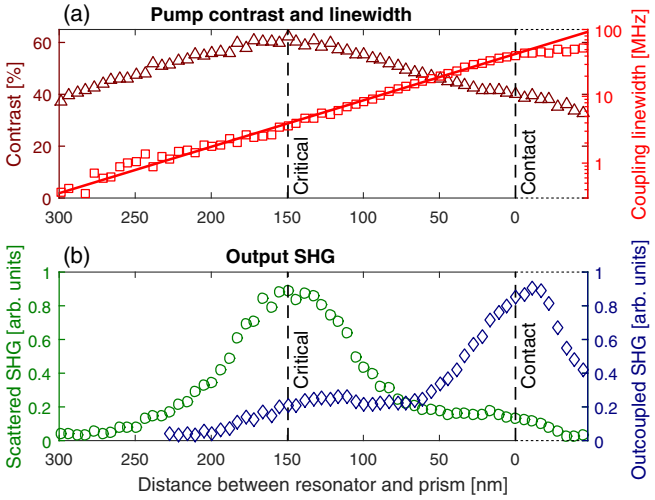


FIG. 1. SHG as a function of the coupler distance. In (a), the pump mode's contrast and linewidth are plotted as the prism is moved closer to the resonator till the two are on contact. At about 150 nm away, the contrast is maximum and the resonance is critically coupled. The behavior of the coupling linewidth changes from exponential at some point. We believe this change is due to contact between the prism and the resonator. Further change on the distance axis is then depression of the resonator by the prism by an unknown amount. Meanwhile, in (b), we measure the second harmonic both scattered from the resonator and coupled out via the prism. The scattered second harmonic gives an indication of the intracavity power. The scattered second-harmonic power reaches a maximum when the prism is critically coupled to the pump, but the outcoupled power follows much later when the signal is better coupled at a closer distance. This is the case even when we believe the prism is depressing the resonator. The method for this experiment is described in detail in Sec. III A.

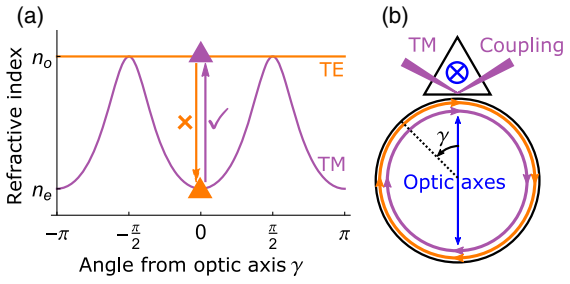


FIG. 2. Selective coupling in a negative uniaxial, $x$-cut WGM resonator. (a) Refractive indices for TE (orange) and TM (purple) modes at different angles, $\gamma$, from the resonator's optic axis, as well as inside a prism for selective coupling made from the same material. This prism is illustrated in (b). It is placed at the resonator's optic axis and has its optic axis perpendicular to that of the resonator. Modes can evanescently couple to a prism if their refractive index inside the prism is greater than or equal to that in the resonator. Therefore, only TM modes can couple to this prism. In a positive crystal, TE modes would couple at this prism.

The TE modes experience the ordinary refractive index, $n_o$ (up to geometric dispersion, which is negligible in our scheme [15]). Meanwhile, TM modes experience an oscillating refractive index between approximately the ordinary and extraordinary refractive indices, $n_o$ and $n_e$. At the two points on the resonator, where the $\mathbf{k}$ vector of the mode is orthogonal to the optic axis, the TM refractive index is purely extraordinary. Here, the difference in refractive indices for the two modes is at a maximum. To utilize this difference, we place a $z$-cut prism of the same negative crystal at one of these points. In this prism, TE and TM modes experience the opposite refractive index of that inside the resonator. For evanescent coupling to occur, the refractive index in the prism must be greater than that in the resonator. As the crystal is negative ($n_o > n_e$), TM modes will couple to this prism, whereas TE modes will not. In positive crystals, TE modes can be selectively coupled in this manner. In our $x$-cut scheme, signal modes are polarized orthogonally to the pump modes. Normal dispersion dictates that, for negative (positive) crystals, these signal modes are therefore TM (TE) polarized. These are precisely the modes we can selectively couple to using the method shown in Fig. 2. We described this scheme in greater detail in Ref. [11].

## III. EXPERIMENTAL RESULTS

In order to experimentally test our hypothesis, we manufacture a 1.2-mm-radius resonator from $x$-cut "optical-grade" congruent LN from MTI Corporation. The resonator is initially sanded on a lathe and then polished with diamond slurry in multiple steps, from 9 $\mu$m down to 0.25 $\mu$m grit size. It has an intrinsic $Q$ factor near 1550 nm of $1.7 \times 10^8$.

The resonator is placed in the experimental setup illustrated in Fig. 3. The pump laser is swept in frequency near 1550 nm and coupled to free space using a pigtailed ferrule and graded index lens. Here, it is internally reflected in a diamond prism, with the normal of its coupling surface parallel to the optic axis of the resonator. The coupling angle is adjusted such that fundamental WGMs are excited efficiently. This diamond prism sits atop a piezoelectric linear stage (Attocube) for control of the coupling distance on the nanometer scale, allowing us to adjust the coupling rate. The reflected light is focused onto an (In,Ga)As detector (Thorlabs) and observed on an oscilloscope. At the used coupling angle, no TM-polarized pump light can couple into the resonator. We therefore adjust the polarization using fiber paddles, such that the resonances have the highest contrast.

When a second harmonic is generated inside the resonator, it can be coupled out of the diamond prism, where it is focused, and reflected by a dichroic mirror—separating pump and signal—onto a Si detector (Thorlabs) for observation. Opposite the diamond prism is a $z$-cut LN prism, which sits atop a second piezoelectric linear stage for independent control of this prism's coupling rate. As

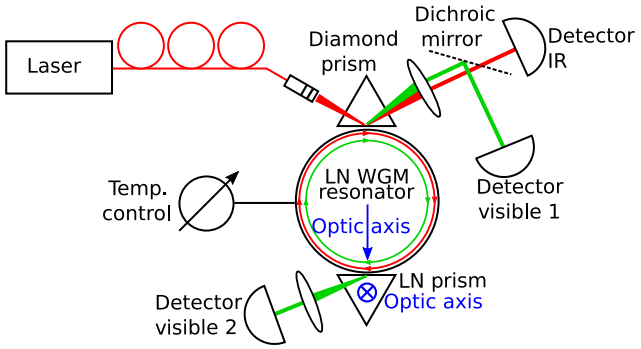


FIG. 3. The experimental setup. Red indicates pump (approximately 1550 nm) light. Green shows the path of the second harmonic when one is generated. Pump light is coupled to an $x$-cut congruent LN WGM resonator using a diamond prism, which can be moved with a piezoelectric linear stage, at the resonator's optic axis. Its reflected spectrum is measured with an (In,Ga)As detector. When second-harmonic light is generated, it can be outcoupled at the diamond prism and measured with a Si detector. In addition, there is a $z$-cut LN prism located opposite to the diamond prism controlled by another piezoelectric linear stage. Second-harmonic (TM-polarized) light can couple out through this prism, but pump (TE-polarized) light cannot.

discussed above, only TM-polarized light can couple to this prism. Light outcoupled there is focused onto a second Si detector (Thorlabs) for observation.

We implement two forms of temperature control. The resonator is surrounded by a resistor-heated temperature-stabilized casing controlled by a proportional-integral-derivative controller. This casing is kept at a stable temperature during the tests, as we wish to keep the resonant frequencies roughly stable. When the diamond and LN prisms are moved to adjust the coupling rates during the tests, they cause dielectric tuning of the modes [14], which changes the phase-matching condition and hence inhibits conversion. To compensate for the changing phase matching, we use a 405-nm laser diode as the fast temperature control. The diode is fiber coupled and shone at the resonator from a bare fiber tip. The up to 5.8 mW of power allows us to tune the pump resonance by about 500 MHz or an equivalent shift to about 1.5 °C of the resistive heating. This illumination does not appear to have any negative effect on the resonator, despite congruent lithium niobate's low optical damage threshold [16–19].

### A. Demonstration of different coupling distances

To show that maximum intracavity SHG—but not maximum outcoupled SHG—is reached when the pump is critically coupled, we use the setup shown in Fig. 3, but with the modification that the LN prism and its detector are replaced simply by a high-gain detector pointed at the resonator and a focusing lens to measure scattered light.

The laser is swept in frequency over a mode at 1548.36 nm. It is maintained at constant power during this test. The reflected spectrum obtained during this sweep allows us to fit the contrast and linewidth of the mode. The pump is initially undercoupled to the point that very little SHG could be measured. The voltage on the piezoelectric stage is increased in 0.1 V steps (about 5.5 nm, estimated from the exponential decay of the linewidth [11]), moving the diamond prism closer to the resonator. At each step, the reflected pump spectrum, as well as the outcoupled and scattered second-harmonic spectra, is recorded. The pump contrast and linewidth are plotted in Fig. 1(a), and the scattered and outcoupled second-harmonic powers in Fig. 1(b). As the detector for the scattered second harmonic can detect only a portion of the total scattered light, the emitted powers are kept in arbitrary units to visualize qualitatively the scaling of powers with coupling. Because of the coupling linewidth's change of growth from exponential at a certain piezoelectric voltage, we believe that a further increase in piezoelectric voltage from that point will cause the prism to squash the resonator. We have taken this point to mean zero distance between the two. Further increase in piezoelectric voltage still increases the coupling linewidth; thus, we continue to take data beyond that point, although we do not know the relationship between a further increase in voltage and the amount the resonator is depressed. We therefore include an uncalibrated negative region on the distance axis.

As can be seen in Fig. 1, the pump contrast increases as the prism is moved closer to the resonator, until it is about 150 nm away. Here, the pump is critically coupled and the scattered second-harmonic power reaches its maximum. This shows that the intracavity SHG is at a maximum at that point. The outcoupled second harmonic, however, is relatively weak until the pump is heavily overcoupled at a much closer distance (even pushing into the resonator). Here, the resonant enhancement of the pump is hindered, causing lower conversion.

### B. Selective coupling

To test selective coupling's efficacy, we first select a conversion channel with high SHG at 1555.4 nm. During this test, the resistive heating is set to 50°C. The laser is swept in frequency around this mode to ensure that the mode volume does not heat up too much due to bulk absorption. The prisms are moved and the modes tuned by controlling the temperature-tuning laser's power until maximum power is coupled out of the LN prism. Here, the pump power is adjusted to measure how the signal power scales with pump power. After these measurements, the LN prism is moved back far enough to ensure that no second harmonic couples out of it. The diamond prism and tuning laser power are then adjusted to obtain maximum power coupled out of the diamond prism, and the pump power is again adjusted to measure the power scaling. The results of these measurements are shown in Fig. 4.

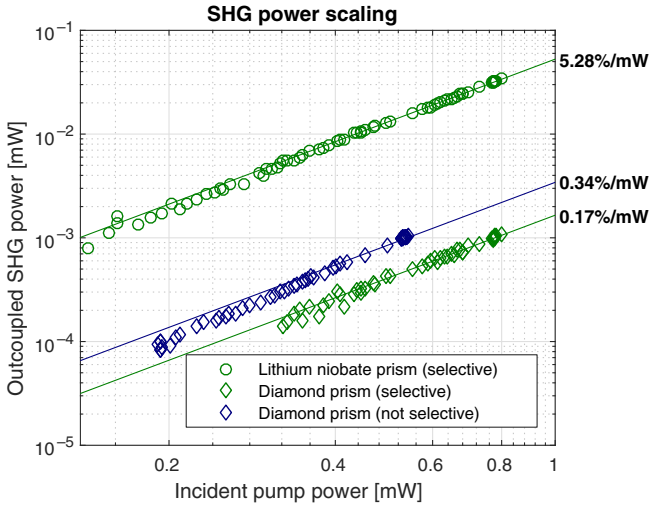


FIG. 4. Second-harmonic (at 777.7 nm) power as a function of pump power. The green markers are measurements where we maximize power selectively outcoupled by the LN prism. The blue markers have power outcoupled by the diamond prism maximized (when no LN prism is present). The LN prism is represented by circles, the diamond prism by diamonds. The linear data for each curve is fitted to a quadratic, and their intercept at 1 mW is labeled. When selective coupling is used, some—but much less—power couples out of the diamond prism. These data are truncated at low SHG power, as their errors approach the noise level.

The detected signal power clearly increases quadratically with pump power in all measurements. Power-law fits of the data (of the form $P_{\mathrm{SHG}} \propto P^{\alpha}_{\mathrm{incident}}$) give $\alpha$ values within 3% of quadratic for the selectively coupled case. For the nonselective case, we find a 14(9)% deviation. This deviation can be explained by the modes slightly detuning from each other at lower power. This quadratic scaling in addition to the wavelength sensitivity range of the Si detectors shows that the signal is the second harmonic. When compared to the "incident power" shown in Fig. 4, the efficiency of SHG without selective coupling is 0.34%, when the fit is constrained to be quadratic. When selective coupling is implemented, there is an efficiency of 5.28% at the selective coupling prism, and 0.17% at the diamond prism. The best possible conversion with the selective coupler is hence 15 times larger than the best possible conversion with a single diamond prism.

Critical coupling of the pump laser in this mode yields the maximum contrast of 40.7%. It is known that $>99\%$ prism coupling efficiency is possible by controlling the ratio of the resonator's radii [20]. As the resonator rim is sanded, we cannot control this ratio; therefore, we scale the incident powers to be 40.7% of the laser power. This scaling is very important for the efficiency measurements, for a somewhat subtle reason. For maximum SHG coupled out of the diamond prism, the pump is overcoupled, meaning that its contrast is lower than 40.7%. A typical contrast in this case is a mere 9%. In this typical case, with 1 mW laser power, 90 $\mu$W is coupled in, but there is 407 $\mu$W incident pump power, which *could have been* coupled in, had the resonance been critically coupled. When selective coupling is used, this extra coupling is achieved; therefore, the extra power is not discounted. Failure to account for power that could have been coupled in would give a conversion efficiency for the nonselective case of 6.53% because, although the second harmonic generated for similar laser powers in that case is 15 times less, the contrast is simultaneously more than 4 times lower. This use of incoupled power when critically coupled is notably different from Refs. [3,9,10], where unadulterated incoupled power is used.

## IV. CONCLUSION

To conclude, we extend the selective coupling of Ref. [11] to uniaxial $x$-cut WGM resonators in this paper. Specifically, we experimentally demonstrate selective coupling to TM second-harmonic modes in a congruent lithium niobate resonator. In this scheme, selective coupling is particularly useful for harmonic generation due to the vastly different coupling distances required for critical coupling. We show both theoretically and experimentally that simultaneous critical coupling of signal and pump modes allows for increased second-harmonic efficiency; because of selective coupling, we are able to increase this efficiency 15-fold. These individually accessible coupling rates will be particularly interesting for applications studying the quantum aspects of nonlinearly generated light in WGMs [21–24]. These results also apply to $z$-cut resonators when an $x$-cut prism is used.

## ACKNOWLEDGMENTS

We acknowledge the extensive support of the Leuchs Division of the Max Planck Institute for the Science of Light, which provided many of the experimental apparatuses used.

[1] P. A. Franken, A. E. Hill, C. W. Peters, and G. Weinreich, Generation of Optical Harmonics, Phys. Rev. Lett. **7**, 118 (1961).

[2] J. U. Fürst, D. V. Strekalov, D. Elser, M. Lassen, U. L. Andersen, C. Marquardt, and G. Leuchs, Naturally Phase-Matched Second-Harmonic Generation in a Whispering-Gallery-Mode Resonator, Phys. Rev. Lett. **104**, 153901 (2010).

[3] J. U. Fürst, K. Buse, I. Breunig, P. Becker, J. Liebertz, and L. Bohatý, Second-harmonic generation of light at 245 nm in a lithium tetraborate whispering gallery resonator, Opt. Lett. **40**, 1932 (2015).

[4] B. Sturman and I. Breunig, Generic description of second-order nonlinear phenomena in whispering-gallery resonators, J. Opt. Soc. Am. B **28**, 2465 (2011).

[5] D. V. Strekalov, C. Marquardt, A. B. Matsko, H. G. L. Schwefel, and G. Leuchs, Nonlinear and quantum optics with whispering gallery resonators, J. Opt. **18**, 123002 (2016).
[6] I. Breunig, Three-wave mixing in whispering gallery resonators, Laser Photonics Rev. **10**, 569 (2016).
[7] T. Beckmann, H. Linnenbank, H. Steigerwald, B. Sturman, D. Haertle, K. Buse, and I. Breunig, Highly Tunable Low-Threshold Optical Parametric Oscillation in Radially Poled Whispering Gallery Resonators, Phys. Rev. Lett. **106**, 143903 (2011).
[8] J. U. Fürst, B. Sturman, K. Buse, and I. Breunig, Whispering gallery resonators with broken axial symmetry: Theory and experiment, Opt. Express **24**, 20143 (2016).
[9] G. Lin, J. U. Fürst, D. V. Strekalov, and N. Yu, Wide-range cyclic phase matching and second harmonic generation in whispering gallery resonators, Appl. Phys. Lett. **103**, 181107 (2013).
[10] G. Lin and N. Yu, Continuous tuning of double resonance-enhanced second harmonic generation in a dispersive dielectric resonator, Opt. Express **22**, 557 (2014).
[11] F. Sedlmeir, M. R. Foreman, U. Vogl, R. Zeltner, G. Schunk, D. V. Strekalov, C. Marquardt, G. Leuchs, and H. G. L. Schwefel, Polarization-Selective Out-Coupling of Whispering-Gallery Modes, Phys. Rev. Applied **7**, 024029 (2017).
[12] M. L. Gorodetsky and V. S. Ilchenko, Optical microsphere resonators: Optimal coupling to high-$Q$ whispering-gallery modes, J. Opt. Soc. Am. B **16**, 147 (1999).
[13] H. A. Haus, *Waves and Fields in Optoelectronics* (Prentice-Hall, Englewood Cliffs, NJ, 1984).
[14] M. R. Foreman, F. Sedlmeir, H. G. L. Schwefel, and G. Leuchs, Dielectric tuning and coupling of whispering gallery modes using an anisotropic prism, J. Opt. Soc. Am. B **33**, 2177 (2016).
[15] I. Breunig, B. Sturman, F. Sedlmeir, H. G. L. Schwefel, and K. Buse, Whispering gallery modes at the rim of an axisymmetric optical resonator: Analytical versus numerical description and comparison with experiment, Opt. Express **21**, 30683 (2013).
[16] M. Leidinger, C. S. Werner, W. Yoshiki, K. Buse, and I. Breunig, Impact of the photorefractive and pyroelectric-electro-optic effect in lithium niobate on whispering-gallery modes, Opt. Lett. **41**, 5474 (2016).
[17] A. A. Savchenkov, A. B. Matsko, D. Strekalov, V. S. Ilchenko, and L. Maleki, Photorefractive effects in magnesium doped lithium niobate whispering gallery mode resonators, Appl. Phys. Lett. **88**, 241909 (2006).
[18] A. A. Savchenkov, A. B. Matsko, D. Strekalov, V. S. Ilchenko, and L. Maleki, Photorefractive damage in whispering gallery resonators, Opt. Commun. **272**, 257 (2007).
[19] A. A. Savchenkov, A. B. Matsko, D. Strekalov, V. S. Ilchenko, and L. Maleki, Enhancement of photorefraction in whispering gallery mode resonators, Phys. Rev. B **74**, 245119 (2006).
[20] D. V. Strekalov, A. A. Savchenkov, A. B. Matsko, and N. Yu, Efficient upconversion of subterahertz radiation in a high-$Q$ whispering gallery resonator, Opt. Lett. **34**, 713 (2009).
[21] M. Förtsch, G. Schunk, J. U. Fürst, D. Strekalov, T. Gerrits, M. J. Stevens, F. Sedlmeir, H. G. L. Schwefel, S. W. Nam, G. Leuchs, and C. Marquardt, Highly efficient generation of single-mode photon pairs from a crystalline whispering-gallery-mode resonator source, Phys. Rev. A **91**, 023812 (2015).
[22] M. Förtsch, T. Gerrits, M. J. Stevens, D. Strekalov, G. Schunk, J. U. Fürst, U. Vogl, F. Sedlmeir, H. G. L. Schwefel, G. Leuchs, S. W. Nam, and C. Marquardt, Near-infrared single-photon spectroscopy of a whispering gallery mode resonator using energy-resolving transition edge sensors, J. Opt. **17**, 065501 (2015).
[23] G. Schunk, U. Vogl, D. V. Strekalov, M. Förtsch, F. Sedlmeir, H. G. L. Schwefel, M. Göbelt, S. Christiansen, G. Leuchs, and C. Marquardt, Interfacing transitions of different alkali atoms and telecom bands using one narrow-band photon pair source, Optica **2**, 773 (2015).
[24] V. Peano, H. G. L. Schwefel, C. Marquardt, and F. Marquardt, Intracavity Squeezing Can Enhance Quantum-Limited Optomechanical Position Detection Through Deamplification, Phys. Rev. Lett. **115**, 243603 (2015).